General Disclaimer

One or more of the Following Statements may affect this Document

DESIGN CONSIDERATIONS FOR
THE AIRFRAME-INTEGRATED SCRAMJET

by John R. Henry and Griffin Y. Anderson

Langley Research Center
Hampton, Va. 23665

DESIGN CONSIDERATIONS FOR THE AIRFRAME-INTEGRATED SCRAMJET[*]

By John R. Henry and Griffin Y. Anderson
Langley Research Center

SUMMARY

Research programs at the NASA Langley Research Center on the development of airframe-integrated scramjet concepts (supersonic combustion ramjet) are reviewed briefly. The design and performance of a specific scramjet configuration are examined analytically by use of recently developed and substantiated techniques on boundary-layer development, heat transfer, fuel-air mixing, heat-release rates, and engine-cycle analysis. These studies indicate that the fixed-geometry scramjet module will provide practical levels of thrust performance with low cooling requirements. Areas which need particular emphasis in further development work are the combustor design for low speeds and the integrated nozzle design.

INTRODUCTION

During the past decade, exploratory research on concepts for hypersonic air-breathing engines has been pursued in substantial research and development programs in the United States, and a considerable technology base has been established. Summaries of this work and the present status of the technology are given in a number of papers. See, for example, references 1 to 3. Several concepts for the supersonic combustion ramjet (scramjet) engine have been shown to be feasible, relative to the aerothermodynamic performance of the engine cycle, by investigations of small-scale research engines and components. (See ref. 1.) Practical levels of performance closely approaching values predicted on the basis of isolated high-efficiency component data have been demonstrated. As part of the research scramjet program in the United States, the NASA has developed the Hypersonic Research Engine (HRE), an axisymmetric dual-combustion mode scramjet engine designed primarily to perform research on the internal aerothermodynamics and to evaluate the fuel-cooled structures design. The structures investigations have been completed successfully, and the aerothermodynamic engine model is now being installed in the ground facility preparatory to extensive performance tests.

The results of the research engine investigations have been used in numerous application studies to evaluate the potential of scramjet propulsion systems for hypersonic

cruise and accelerating missions, for instance, the air-breathing launch vehicle study of reference 4. These studies forecast superior performance for hydrogen-burning hypersonic air-breathing systems (ref. 5) providing that sufficient technology is developed in certain key areas, particularly structures, heat protection, and airframe-integrated propulsion systems, as outlined in references 2, 6, and 7. Although exploratory research on propulsion integration for hypersonic vehicles has been in progress in a number of organizations, particularly for the subsonic combustion ramjet (ref. 8), there still is a need for scramjet engine concepts which will integrate geometrically and aerodynamically with a vehicle configuration and provide high performance and satisfactory operating characteristics over the flight speed ranges; these considerations extend beyond the goals of the research engine investigations and represent major achievements which have to be accomplished prior to the realization of practical operational vehicles.

The Langley Research Center of the NASA also has initiated a research program which is focused on the development of integrated scramjet concepts and which is coordinated with similar NASA programs in the structures and vehicle aerodynamics areas. Promising approaches to the engine design problem are beginning to emerge from this work, as described in reference 9, where it is noted that a principal guideline is the achievement of designs which have an engine structure cooling requirement equivalent to only a fraction of the total fuel heat sink available. The realization of this goal will provide the vehicle designer with a much broader range of approaches since he will be able to employ the excess heat sink for actively cooled vehicle structures and avoid many of the problems of hot structures and the associated aerodynamic disadvantages (ref. 9). This paper will describe some of the initial work in the integrated scramjet programs and also the present design approaches. A scramjet concept now under study at Langley will be analyzed in detail relative to component and overall performance and to operating characteristics, and comparisons will be made with a baseline performance obtained by use of typical engine cycle assumptions. The main consideration in the present study is the question: "If the undersurface of the vehicle is used effectively to perform inlet and exhaust nozzle functions, can the relatively small fixed-geometry engine module provide the desired levels of thrust and low cooling characteristics?"

SYMBOLS

Measurements and calculations were made in U.S. Customary Units. They are presented herein in the International System of Units (SI) with the equivalent values given parenthetically in the U.S. Customary Units.

A_1 capture area

A_2 inlet throat area

A_3 combustor exit area

A_∞ area of free-stream tube

A_C cowl area

A_N nozzle exit area

C_T thrust coefficient

h height of engine at cowl

I_{SP} specific impulse

K pressure area integral factor

L relative length of combustor

M Mach number

M_∞ free-stream Mach number

p pressure

p_2 inlet pressure

p_3 combustor pressure

q_∞ dynamic pressure in free stream

T_W wall temperature

x/x_1 fraction of mixing length

δ turning angle through a shock

η_C chemical combustion efficiency

η_K kinetic energy available by isentropic expansion from throat conditions to initial pressure divided by initial kinetic energy in the free stream

η_{KN} kinetic energy efficiency of nozzle

ϕ equivalence ratio

SCRAMJET DESIGN AND PERFORMANCE

General Features of Integrated Concepts

Airframe-engine integration.- The type of propulsion system installation under consideration is illustrated by the lifting-body concept for an air-breathing launch vehicle (ABLV) given in figure 1 (taken from ref. 4). This concept is defined as a horizontal take-off and landing (HTOL) vehicle capable of relatively normal "airline-type" operations with reusability of both stages and a take-off gross weight of 4448 kN (10^6 lb). Engine modules are mounted side by side on the underside of the vehicle toward the aft end. Vehicles with actively cooled structures designed for cruise in the Mach 6 to 8 range might be considerably smaller and more conventional looking (ref. 5), but the main features of the propulsion system installation would be similar. From figure 1, it is clear that the entire underside of the vehicle becomes involved in processing the engine airflow. The reason for this blending of the vehicle and engine functions is the well-known fact that at hypersonic speeds very large engine airflows are required for adequate thrust in spite of the high-energy potential of the hydrogen fuel. Under these circumstances, practical configurations result in major parts of the vehicle serving as engine hardware.

These design features are illustrated more clearly by the sketch in figure 2. Before entering the engine module inlet, the airflow is compressed by the shock produced by the bow of the vehicle. This feature not only reduces the compression required by the inlet but also reduces the physical size of the engine module needed to produce the required thrust by about a factor of 3 at Mach 10. The space available for the propulsion system located between the vehicle undersurface and the bow shock, as shown in the cross section, is several times wider than it is high; this geometry suggests the arrangement of several rectangular engine modules side by side. The modular concept also has the important fringe benefit of permitting engine development in ground facilities of practical size. An unfavorable aspect of the design is the relatively thick turbulent boundary layer generated on the forebody of the vehicle, which must be ingested by the engines in practical designs. The effects of this design aspect are discussed later in the paper.

The other major geometric design feature of the integrated configuration which is external to the engine modules is the vehicle afterbody, which is used as an extension to the engine nozzle. This feature permits much higher effective engine exhaust velocities with relatively modest area expansions in the module nozzle hardware itself and with low engine external drag. The technology required to design the aft end of the vehicle to serve

the thrust function requires further development and refinement because of the complex aerodynamic situation. For example, the flow may be three-dimensional, off-design operating conditions could induce boundary-layer separation, the gross thrust vector at high flight speeds will be large compared with the net thrust, and a misalinement of the vector could produce large trim penalties. However, the performance advantages are great enough to warrant the development effort.

The advantages of the integration concepts illustrated in figure 2 are expressed quantitatively in figure 3 which presents a breakdown of typical values of thrust coefficient computed for a Mach number range from 4 to 10. A vehicle forebody shock corresponding to a turning (δ) of 8° was assumed; this compression is responsible for a thrust contribution of about 35 percent, primarily because of the increased mass flow per unit area at the engine face. For the afterbody, the effective nozzle exit area was assumed to be 2.8 times the flow area at the engine cowl; this extra expansion produces thrust contributions ranging from about 25 to 35 percent, depending on the Mach number. This contribution is due to the improved cycle performance or specific impulse.

Engine module arrangement.- In order to accelerate the vehicle from take-off to hypersonic speeds, the propulsion system must provide adequate thrust up to the Mach 3 to 4 range where the dual-combustion-mode scramjet becomes effective. A number of solutions to this problem are possible, including compound and composite engines (ref. 2); for the purposes of this paper, it is assumed that turbojet engines will perform this function. On this basis the engine module might have the arrangement shown in the sketch of figure 4. The turbojet and its ducting are embedded in the body of the vehicle with the scramjet engine mounted underneath. A variable-geometry inlet and adjustable door would be required to match the airflow requirements of the turbojet. The adjustable door would also be used to close off the turbojet ducting above the Mach 3 to 4 range, where the scramjet would provide the entire thrust. For the present time it is assumed that there is no requirement to close off the scramjet (ref. 9) although this could be done if needed.

A fixed-geometry scramjet is shown in the sketch; this engine is the main object of a research program at the Langley Research Center, and it will be used to illustrate the approaches to an integrated design later in the paper. It is appropriate at this point to determine quantitatively the performance losses associated with the assumption of fixed geometry. The scramjet engine basically should operate at high inlet area contraction ratios at high flight speeds in order to keep the velocities in the combustor at the low levels required for low momentum losses and high thrust. In contrast, fixed-geometry inlets are limited relative to maximum contraction ratio because the inlet must have the capability of starting or establishing supersonic flow in the inlet at the low end of the Mach number range. Therefore, the inlet throat probably is the leading candidate for variable geometry.

This question has been evaluated by performing engine cycle analyses for an assumed flight trajectory corresponding to a free-stream dynamic pressure of 47.9 kN/m^2 (1000 psf), typical values of component efficiencies and inlet flow spillage, a vehicle bow shock with a turning of 8°, and a stoichiometric fuel-air ratio ($\phi = 1.0$). The results are given in figure 5 in terms of specific impulse as a function of flight Mach number. For the fixed-inlet geometry, contraction ratios ranging from 6 to 10 were assumed to be possible, depending on the inlet design. With variable geometry, a high contraction ratio value of 25 was assumed for the Mach range from 8 to 10, the value decreasing as the Mach number is reduced below 8 in order to avoid choking the inlet throat. (See dashed curve in fig. 5.) The results indicate that variable geometry would increase the performance by a maximum of only 16 percent. The associated penalty would be increased system complexity and seal and joint problems. In addition, at high contraction ratios it would be very difficult to cool the engine within the heat-sink limits of the fuel because of the increased internal pressures. All these penalties would involve increases in weight which would tend to cancel the performance increase. In view of these results, the conclusion is that variable scramjet geometry does not appear to be justified in the present early stages of the development work.

Langley Scramjet Analyses

Baseline assumptions.- Performance analyses for the specific geometric and operating features of an integrated scramjet concept under study at Langley are compared with baseline values for engine cycle performance; these values are believed to be typical on the basis of past studies and are required to produce a reasonable goal. Figure 6 summarizes the baseline assumptions. For this accelerating mission the equivalence ratio is 1.0, and for simplicity the turning through the vehicle bow shock is assumed to be constant at 8°. The fixed-geometry scramjet module has a fairly optimistic inlet contraction ratio of 10 with an inlet kinetic energy efficiency of 0.97, a combustion chemical efficiency of 0.95, and a nozzle kinetic energy efficiency of 0.99 to 0.98, frozen flow being assumed. The effective nozzle exit area is 2.8 times the cowl area; this assumption may be conservative, depending on the vehicle design.

Specific impulse values corresponding to these assumptions are given in figure 7 where they are shown to compare reasonably well with a band of values taken from studies in the literature. In addition, the baseline performance lies roughly in the middle between the goal and minimum values specified for the NASA Hypersonic Research Engine. From figure 7 it is concluded that the baseline performance is reasonable and representative. Corresponding values of thrust coefficient have been given by the top curve of figure 3.

Langley scramjet concept.- A sketch representing an oblique view of the current design for the Langley scramjet is given in figure 8. Three design requirements have led

to the evolution of this type of configuration: fixed geometry, low cooling, and the shape of the space between the vehicle bow shock and vehicle undersurface available for locating the engine modules. Fixed geometry dictates that the sidewall leading edges must have sweep to provide an open "window" upstream from the cowl leading edge to spill flow downward during the inlet starting process at the low end of the Mach number range. Throughout the engine, planes of constant flow properties tend to be parallel to the swept leading edges; therefore, the fuel injection struts are swept at the same angle. As noted previously, modules of rectangular cross section utilize efficiently the engine air capture area available on the vehicle. Low cooling requirements dictate low wetted area in the combustor which, in turn, requires fuel injection from multiple planes in the stream to obtain short mixing and combustion lengths. This condition is accomplished by injecting fuel from rows of discrete orifices on both sides of each of the three struts. The configuration is in the early stages of development. Several inlet investigations have been completed and have led to the present design; work on the combustor and the nozzle development has been initiated. Many of the present design features are expected to change to some extent as the work progresses.

Design features for reduced cooling requirements.- Thermal-protection systems for the scramjet engine normally will be of the regenerative type, the internal walls formed by cooling jackets or tubes through which cold fuel will be circulated to absorb the heat. The heated fuel then will be injected into the airstream and burned; thus, the heat transferred through the engine walls is conserved. Typical designs and weights for the sandwich-fin type of heat exchanger are discussed in reference 1. The current state of the technology for this type of cooled structure does not permit adequate cycle life for practical engines; this problem and approaches to solving it are discussed in reference 7.

The two principal approaches to reducing the engine cooling requirements are the reduction of the wetted wall area and the reduction of the heat-transfer rate, particularly in the combustor. A new method has been developed at Langley for estimating heat transfer in the supersonic combustors based on a modification and extension of the method of reference 10. An integral boundary-layer technique is used that has provisions for the effects of pressure gradient and nonequilibrium velocity distributions on boundary-layer growth and heat transfer. The accuracy of the method has been substantiated by comparisons with heat-transfer data (ref. 11) measured in supersonic combustors. The method has been used in analyses to illustrate the effectiveness of several design techniques in reducing cooling requirements; the results are given in figure 9.

Figure 9(a) illustrates the reduction in combustor cooling requirement obtainable by the use of struts. Since the mixing length, and therefore the combustor length, is proportional to the gap between the struts, the use of up to three struts produces large reductions in wetted area. Figure 9(b) indicates a large reduction in cooling requirement produced

by the use of supersonic combustion instead of subsonic for a flight Mach number of 6. Either case would produce about the same thrust but supersonic combustion would produce lower pressures and heat transfer in the combustor. Figure 9(c) illustrates a savings produced again by reducing the pressure in the combustor through the use of larger area ratios, with some sacrifice in thrust. All these features have been utilized in the Langley scramjet design.

Inlet performance.- The present concept for the inlet of the Langley scramjet (fig. 8) has a leading-edge sweep angle of 48° for the sidewall compression surfaces, which have wedge angles of 6° in the flow direction. Analyses of experimental data on a similar inlet design indicate that for the current design, the leading edges of the struts should have attached shock waves to a Mach number just under 4, that the shock strengths are low and no boundary-layer separation should occur, and that the inlet should start at a Mach number of about 3.0.

A typical shock diagram is given in figure 10. The internal compression is divided between the sidewalls and front surfaces of the struts. With this type of design, it is impossible to prevent the sidewall shocks from merging with the strut shocks at some flight speed. This situation is relieved by changing the wall slope of the struts and thereby either canceling a shock or reducing the shock strength, as noted in the figure. The sweptback shock waves in this type of inlet design (fig. 10) turn the flow slightly downward as well as in the direction indicated on the diagram; therefore, the minimum flow area between the struts cannot be readily defined by any physical plane. Consequently, the effective inlet area contraction ratio is defined by the flow process which produces the Mach number change throughout the inlet, a contraction ratio value of 8.7 in this case. The higher contraction ratio value of 10 assumed for the baseline performance has not yet been demonstrated to be feasible in the experimental programs for a fixed-geometry inlet of this type.

The performance of the Langley scramjet inlet has been estimated by use of real-gas shock relations for the inviscid flow (fig. 10) and the real-gas boundary-layer method described in a previous section The analysis assumed the same flight trajectory as the baseline performance and a vehicle with a take-off gross weight of 4448 kN (10^6 lb) for which the engine module inlet was located 55 meters (180 ft) downstream of the nose of the vehicle. The inlet was 2.44 meters high by 1.95 meters wide (8 ft by 6.4 ft). The total-pressure recoveries in the inlet throat in the boundary layer and in the inviscid flow were mass weighted and converted to an overall kinetic energy efficiency η_K. The results are given in figure 11.

The kinetic-energy efficiency of the Langley scramjet inlet is predicted to be above 0.98 and above the baseline except at Mach 4 where it drops to a value of 0.974. At Mach 4

the inlet flow spillage is relatively high, 33 percent; therefore, the flow in the throat contains a large amount of boundary layer which originated on the vehicle forebody. As a consequence, the efficiency is lower. For comparison, a simple two-dimensional inlet was designed without sweep and its performance was predicted. The efficiencies were nearly identical to those of the Langley inlet; however, variable geometry would be required to start the inlet and to spill enough flow at Mach 4 to avoid choking the throat.

Flow capture ratios also were computed and are presented in figure 11. The values compare well with experimental data obtained on a similar inlet with a sweep angle of 56°. Some discrepancies are to be expected below a Mach number of 5.3 where the 56° model had detached shock waves at the strut leading edges. The baseline and two-dimensional design cases required more spillage at lower Mach numbers to avoid choking the throat at a geometric contraction ratio of 10. At the higher Mach numbers, the capture ratio of the Langley inlet approaches 0.95, instead of 1.0, because the leading edge of the cowl is downstream of shocks produced by the sidewall compression surfaces (fig. 8). However, in general, the capture ratio schedule is as high as is practical with the amount of internal contraction ratio provided by the inlet.

The contributions of the inviscid and boundary-layer flows to inlet efficiency losses are given in figure 12 together with boundary-layer thickness contours in the throat for a typical case. The relatively small effect of the boundary layer on the efficiency over most of the Mach number range indicates that high accuracy for the boundary-layer predictions was not required. However, reference 10 and further comparisons with unpublished d a using the modified version of the method provide a high degree of confidence in the predictions. The inviscid efficiency data for the inlet with a 56° sweep lie generally below the curve for the current analysis because the compression shocks in the inlet were stronger. In the sketch of the inlet throat, the scale of the width is five times that of the height; therefore, the boundary-layer thickness on the top surface, which originated on the forebody of the vehicle, is several times that of the other boundary layers. In order to avoid subjecting the top boundary layer to strong adverse pressure gradients, the top surface has been designed to follow streamlines when the Mach number in front of the inlet is 6. Since the downward turning for sweptback shocks increases as the Mach number is reduced, this design produces small amounts of expansion turning originating on the top surface at Mach numbers below 6 and slight amounts of compression at Mach numbers above 6. This type of design has been substantiated experimentally.

Combustor design and performance.- Some principal features of the combustor design concept, including some advantages of struts for fuel injection, have already been outlined. Additional constraints are imposed on the combustor configuration by other factors. An important constraint results from the intention to operate with fixed geometry and supersonic flow in the combustor (at least in a one-dimensional sense) at low flight

Mach numbers. In order for this to be possible, rather large combustor area ratios are required. Figure 13 presents the required combustor area ratio as a function of the amount of heat addition in a constant Mach number process. Conditions for the calculations are representative of Mach 4 flight with wall friction effects included. The required area ratio approaches 7 for stoichiometric heat addition. It should also be noted that figure 13 implies a requirement for a relation between area distribution and heat release at low flight Mach numbers to maintain supersonic flow.

In discussing cooling requirements, the point was made that increased combustor area ratio leads to lower combustor cooling requirements. (See fig. 9.) However, this reduced cooling requirement is accompanied by some reduction in engine performance. Figure 14 indicates the magnitude of cooling reduction and performance loss for conditions typical of Mach 10 flight. An increase in the combustor area ratio from a value of 2 to a value of 5 produces a 20-percent reduction in the heat load with only a 3-percent loss in impulse. However, this result is for an exponential heat-release distribution in the combustor which provides most of the heat release close to the injectors. A linear heat-release distribution in the same geometry further reduces the cooling requirements but with a large loss of impulse. Thus, not only the combustor geometry but also the heat-release distribution produced by the fuel injector design is important in determining the engine cooling requirements and performance.

One way to approach describing the relation between fuel injector design and heat-release distribution is to develop means to describe the rate of fuel-air mixing in terms of injection conditions and geometry. If the flow pressure and temperature are high enough to insure rapid chemical reaction, the rate of heat release will be the same as the rate of mixing. Figure 15 presents the variation of the relative amount of mixing with distance for perpendicular wall injection and parallel instream injection derived from nonreactive hydrogen-air mixing experiments. For perpendicular injection, the distribution is based on measurements made downstream of a row of circular sonic orifices. (See ref. 12.) Integrations of detailed flow surveys were used to arrive at a "mixing efficiency" defined as the fraction of fuel mixed with air so that it would react if complete reaction occurred without further mixing. The band of values corresponds to the small variation produced by changing from a close to a wide injector spacing. In the region close to the injector, the composition measurements probably represent the distribution of lumps of fuel rather than the molecular scale mixing needed for chemical reaction. (See refs. 13 and 14.) The amount of mixing near the injector was arbitrarily reduced to account for this lack of molecular mixing as shown by the dashed line in figure 15.

An example of the usefulness of this approach is shown in figure 16 where combustor static-pressure distributions predicted with the mixing efficiency correlation are compared with data from reference 11. The theoretical calculations represented by the solid

10

line were made with a one-dimensional real-gas analysis in which chemical reaction is distributed with length according to the mixing distribution for perpendicular injection shown in figure 15. Agreement with the data and the theoretical calculation of reference 11 in the diverging part of the combustor is quite good. No attempt was made to model the separation near the injector. A further comparison with data is shown in figure 17 where the fraction of fuel burned, measured at the exits of a wide variety of experimental combustors, is plotted against the predicted fraction of fuel mixed, calculated with the mixing efficiency correlation. Agreement is generally within ±0.1. This amount of scatter is quite acceptable since the mixing efficiency correlation ignores a number of secondary effects on mixing such as pressure gradient, chemical reactions, combustor design details, and so forth.

The mixing efficiency distribution for parallel instream injection also is shown in figure 15. The variation for a single injector is based on calculations made with the analysis of reference 15 by use of the turbulent eddy viscosity model described in reference 16. It is interesting to note that for a single parallel injector, the amount of mixing is very nearly linear with length. Of course, in a combustor multiple fuel jets would be used, and the merging and subsequent mixing of fuel patterns from adjacent injectors become important. The effect of merging for a uniformly spaced array of parallel jets is shown by the top curve in figure 15. The calculations were performed by the analysis presented in reference 17 and by using the eddy viscosity model of reference 16. Note that the length scale is nondimensionalized by the length for complete mixing. For a given size for the injectors, the merging of the mixing patterns increases the absolute length for complete mixing; however, the use of the nondimensional length parameter for figure 15 raises the multiple-jet mixing efficiency curve above the single-jet curves.

A comparison of the single-jet mixing efficiency theory with data is presented in figure 18. The static pressure in a constant-area duct with parallel injection of hydrogen on the center line is compared with the static pressure predicted by a one-dimensional analysis. The chemical reaction distribution with length was assumed to be linear, and the analysis is the same as that used for the calculations presented in figure 16. Again, agreement with the data is good. It is concluded that a mixing efficiency estimated from cold-flow mixing experiments can be quite useful in predicting the heat-release distribution produced by fuel injectors in supersonic combustors.

By use of the design tools just described, a combustor and strut injector design for the Langley scramjet has been defined as shown in figure 19. This design is based on the assumption that all fuel is injected from the struts and that the exit of the combustor has a square cross section. Wall angles are generally less than 6° from the flow center line. The struts may appear to have a rather high blockage (about 60 percent of the entrance area); however, this factor is relieved by the sweep. This type of geometry results from

the requirements that the upstream part of the struts performs a significant amount of the inlet compression process and that the strut cross section must be large enough to carry all the engine fuel to the injectors at reasonable pressures.

The one-dimensional area distribution for the geometry of figure 10 is presented in figure 20. Since there are multiple flow passages in the strut region, the rate of change of area with length is greater there than in the downstream section of the combustor even though the wall angles are about the same. A procedure for matching the heat-release schedule to the area distribution to avoid choking at low flight Mach numbers is also indicated. By selecting the proper injector diameter and conditions, the downstream slope of the area distribution can be matched with heat release by using parallel injectors located on the struts. This part of the heat release is shown by the broken line in figure 20. The steeper slope in the strut region can be approximated by perpendicular injection from the struts at the proper conditions. The resulting overall heat-release schedule is assumed to be the sum of the perpendicular and parallel injection contributions and is shown by the long-dashed line in figure 20. The overall heat release closely approximates the one-dimensional area distribution. Theoretically, a perfect match would given nearly constant Mach number heat addition as assumed in figure 13. The overall combustor area ratio arbitrarily has been limited to a value of 5 as a reasonable compromise between low- and high-speed requirements. As a consequence, the operating fuel-air ratios are less than stoichiometric ($\phi < 1.0$) below a flight Mach number of 5.5. The effect of this condition on performance will be evaluated in a later section of the paper.

Of course, at higher flight Mach numbers where choking is not a problem, all the fuel can be injected perpendicular to the flow to achieve the most rapid heat release and highest specific impulse. A measure of the relation between area distribution and heat-release schedule is the integral of the wall pressure. The calculated values of this pressure integral for the geometry and heat release of figure 20 are shown in figure 21 in dimensionless form as a function of flight Mach number. As indicated by the scale at the right of the figure, the higher the combustor wall pressure integral or "thrust," the higher the resulting engine performance. At low flight Mach numbers, values of pressure integral factor less than 1 result for constant Mach number heat addition. In the baseline performance evaluation, for simplicity the value of the pressure integral factor was assumed to be 1.0; figure 21 shows this assumption to be unrealistic over most of the Mach number range.

A concept for a combustor which has the potential for operating from Mach 4 to 10 with all supersonic combustion and with all the fuel injected for the strut station has been discussed briefly. It will be noted later that high performance and low cooling requirements are predicted for the configuration. Other approaches to the low-speed design are possible, such as additional fuel injection stations downstream on the sidewalls and the use

of the subsonic combustion mode. These features were not discussed here because the analytical difficulties preclude the development of meaningful results. The present design and variations of it are being evaluated experimentally.

Nozzle design and performance. - In order to complete the analysis of the engine performance and operating characteristics, a simple two-dimensional nozzle has been designed and performance predictions have been made by using real-gas analyses for both the inviscid and boundary-layer flows. (See fig. 22.) Most of the nozzle is located in the vehicle afterbody, and the effective exit area was assumed to be 2.84 times the projected frontal area of the inlet, as in the baseline configuration. A conservative value of 15.1^0 for the maximum wall slope on the upper surface was selected to insure flow uniformity; thus, a rather long nozzle was produced, 10 times the projected frontal height of the engine (10h). The nozzle probably can be made much shorter; however, this determination should be made by an optimization process in which many factors are considered, including the nozzle thrust performance over the speed range, the nozzle cooling requirements, and the integration with the vehicle aerodynamic performance relative to parameters such as lift and trim drag. The results of a preliminary study of the effects of the propulsion system on the vehicle aerodynamics is given in reference 18; however, more in-depth analyses and much technology development remain to be accomplished. Such work is beyond the scope of this paper. Therefore, the simple approach illustrated in figure 22 has been taken.

The comparison between the baseline and predicted kinetic energy efficiencies indicates that there is no significant difference, on the order of a maximum of 20 seconds in specific impulse. The efficiency parameter reflects the thrust losses produced by the boundary-layer growth; the analysis also accounts for another major loss through the assumption of frozen flow at the nozzle entrance. Analyses of the flow kinetics (ref. 18) indicate that this assumption is conservative.

Engine cooling requirements.- The results of the boundary-layer predictions in terms of cooling required by the engine referenced to the heat sink available in the hydrogen fuel are given in figure 23. As one might expect, the combustor and nozzle components require the most cooling. One goal of the research program will be to reduce the length of these components and the associated cooling requirement. However, the present analysis predicts substantial amounts of excess heat sink available for actively cooled structures on the vehicle over the entire flight Mach number range considered. It should be noted that the heat-transfer analysis for simplicity was based on a uniform hot wall temperature of 1100 K; advanced designs for cooling circuits, which have yet to be developed, would be required to approach this condition. On the other hand, the successful development of insulation techniques or coatings would permit significant reductions in the cooling load.

The sensitivity of the cooling requirement to the uniformity of the wall temperature was explored by repeating the analysis at the high end of the Mach number range for the arbitary assumption that the hot wall varied in temperature from a value of 330 K near the leading edge of the inlet to a high of 1100 K in the combustor to 500 K at the end of the nozzle. As noted in figure 23, the effect was to increase the total cooling required by only about 15 percent.

Thrust performance prediction.- The performance of the Langley scramjet has been predicted with values of component efficiency data and other parameters derived from the analyses just described. Specific impulse and thrust coefficient values are compared with the baseline in figure 24. Clearly, the two sets of curves are very close in both cases, the Langley engine providing 2 to 3 percent less thrust. A few points, however, should be noted. In the range of Mach 4 to 5, the present combustor concept requires an equivalence ratio of less than 1.0 to avoid thermal choking with all supersonic combustion. This condition produces higher values of specific impulse and lower thrust coefficients. The thrust at Mach 4 could be increased appreciably by the use of an equivalence ratio of 1.0 with subsonic or mixed supersonic and subsonic combustion. The performance with these modes of combustion has to be determined experimentally. The inclusion of combustor wall friction and accurate evaluations of the combustor-wall pressure-area integral for the Langley engine predictions produced more realistic answers than for the baseline. The inlet flow capture, which has a direct proportional effect on thrust, is higher for the Langley scramjet below Mach 6.5. However, the inlet spills 5 percent of the flow at Mach 10 and the thrust is reduced a like amount; whereas the baseline case had no spillage at Mach 10.

CONCLUDING REMARKS

The Langley research program on the development of airframe-integrated scramjet concepts is in an early stage; therefore, the examination of the principal design features of the engine and the forecasts of performance have been slanted generally toward the conservative approach. The definition of the design of the components either has been based on experimental data in hand in the case of the inlet, or on well-founded design techniques in the case of the combustor, or on a simplified design in the case of the nozzle. The central consideration involves the adequacy of thrust performance obtainable with a fixed-geometry scramjet engine module used in conjunction with the undersurface of the vehicle to perform part of the inlet and nozzle functions. A design criterion of equal importance is a low engine cooling requirement which corresponds to a fraction of the heat sink available in the hydrogen fuel; this characteristic will provide the option of fuel-cooled structures for the airframe.

The principal features of the Langley scramjet concept are the sweptback inlet compression surfaces, multiple planes of fuel injection from sweptback struts, multimode fuel injection for efficient operation over the Mach number range, and an unsymmetrical nozzle. Detailed analyses which used recently developed techniques do predict high levels of performance and low cooling; areas needing particular emphasis in further development work are the combustor design for low speeds and the integrated nozzle design.

Langley Research Center,
    National Aeronautics and Space Administration,
        Hampton, Va., September 20, 1973.

REFERENCES

1. Henry, J. R.; and McLellan, C. H.: Air-Breathing Launch Vehicle for Earth-Orbit Shuttle — New Technology and Development Approach. J. Aircraft, vol. 8, no. 5, May 1971, pp. 381-387.

2. Henry, John R.; and Beach, H. Lee: Hypersonic Air-Breathing Propulsion Systems. Vehicle Technology for Civil Aviation — The Seventies and Beyond, NASA SP-292, 1971, pp. 157-177.

3. Ferri, A.: Review of Scramjet Propulsion Technology. J. Aircraft, vol. 5, no. 1, Jan.-Feb. 1968, p. 3.

4. Gregory, T. J.; Williams, L. J.; and Wilcox, D. E.: Airbreathing Launch Vehicle for Earth Orbit Shuttle — Performance and Operation. J. Aircraft, vol. 8, no. 9, Sept. 1971, pp. 724-731.

5. Becker, John V.; and Kirkham, Frank S.: Hypersonic Transports. Vehicle Technology for Civil Aviation — The Seventies and Beyond, NASA SP-292, 1971, pp. 429-445.

6. Bushnell, Dennis M.: Hypersonic Airplane Aerodynamic Technology. Vehicle Technology for Civil Aviation — The Seventies and Beyond, NASA SP-292, 1971, pp. 63-84.

7. Anderson, Melvin S.; and Kelly, H. Neale: Structures Technology for Hypersonic Vehicles. Vehicle Technology for Civil Aviation — The Seventies and Beyond, NASA SP-292, 1971, pp. 179-192.

8. Bourgeois, Jean-Pierre; and Chiché, Fabien: Some Aerodynamic Problems Related to the Propulsion of a Hypersonic Aircraft. NASA TT F-10,944, 1967.

9. Becker, John V.: Prospects for Actively Cooled Hypersonic Transports. Astronaut. & Aeronaut., vol. 9, no. 8, Aug. 1971, pp. 32-39.

10. Pinckney, S. Z.: Method for Predicting Compressible Turbulent Boundary Layers in Adverse Pressure Gradients. NASA TM X-2302, 1971.

11. Billig, Frederick S.; and Grenleski, S. E.: Heat Transfer in Supersonic Combustion Processes. Paper presented at Fourth International Heat Transfer Conference (Versailles, France), Aug. 1970.

12. Rogers, R. Clayton: Mixing of Hydrogen Injected From Multiple Injectors Normal to a Supersonic Airstream. NASA TN D-6476, 1971.

13. Hottel, H. C.; and Williams, G. C.: Measurements of Gas Composition (section C,6, pp. 62-73) and Measurement of Time-Dependent Properties (section C,8, pp. 82-88). Design and Performance of Gas Turbine Power Plants, W. R. Hawthorne and W. T. Olson, eds., Princeton Univ. Press, 1960.

14. Anderson, Griffin Y.; Agnone, Anthony M.; and Russin, Wm. Roger: Composition Distribution and Equivalent Body Shape for a Reacting, Coaxial, Supersonic Hydrogen-Air Flow. NASA TN D-6123, 1971.

15. Diffusion Controlled Combustion for Scramjet Application. Tech. Rep. 569 (Contract No. NAS 1-5117), Gen. Appl. Sci. Lab., Inc., Dec. 1965.
    Edelman, R.: Pt. I — Analysis and Results of Calculations. (Available as NASA CR-66363.)
    Hopf, H.; and Fortune, O.: Pt. II — Programmer's Manual. (Available as NASA CR-66714.)

16. Eggers, James M.: Turbulent Mixing of Coaxial Compressible Hydrogen-Air Jet. NASA TN D-6487, 1971.

17. Alzner, Edgar: Three Dimensional Mixing of Jets. ATL TR 150 (Contract NAS 1-9560), Advanced Technologies Lab., Inc., July 1970. (Available as NASA CR-111782.)

18. Johnston, P. J.; Cubbage, J. M.; and Weidner, J. P.: Studies of Engine-Airframe Integration on Hypersonic Aircraft. J. Aircraft, vol. 8, no. 7, July 1971, pp. 495-501.

Figure 1.- Air-breathing launch vehicle concept. (From ref. 4.)

L-73-6878

THRUST

ENGINE MODULES

SCHEMATIC OF
ENGINE CROSS SECTION

SHOCK

SHOCK
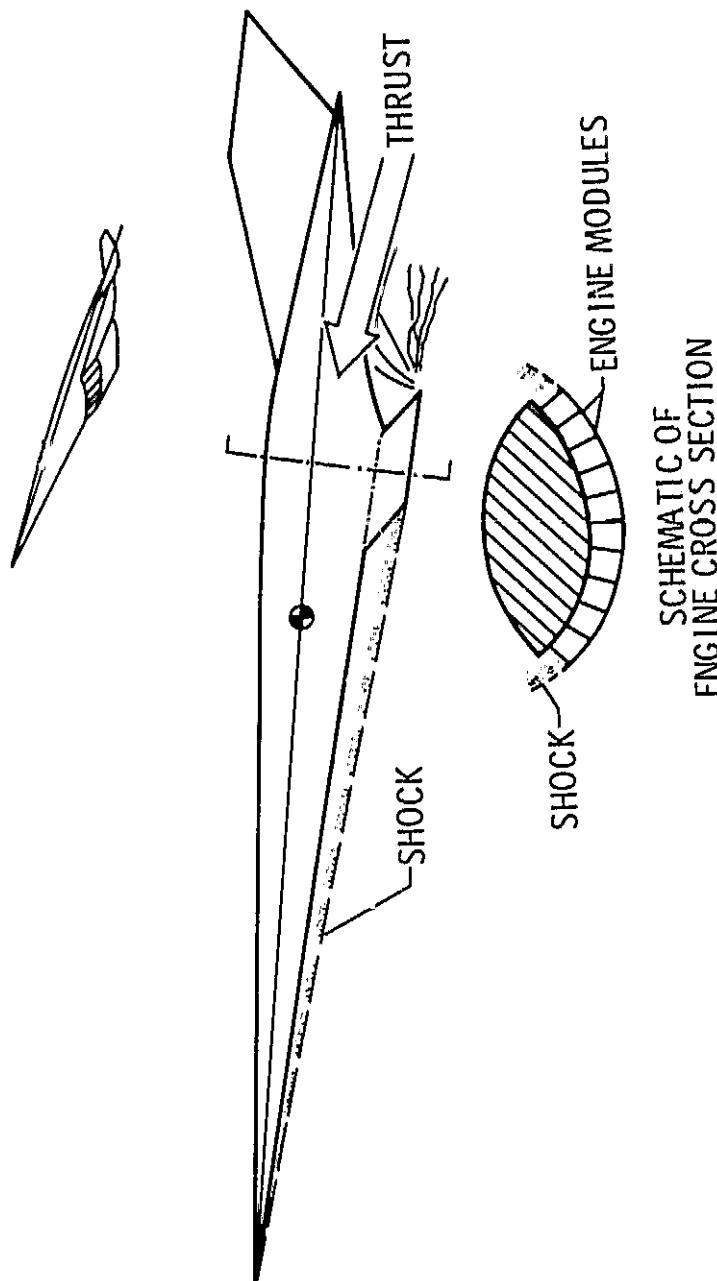
Figure 2. - Scramjet-vehicle integration.

19
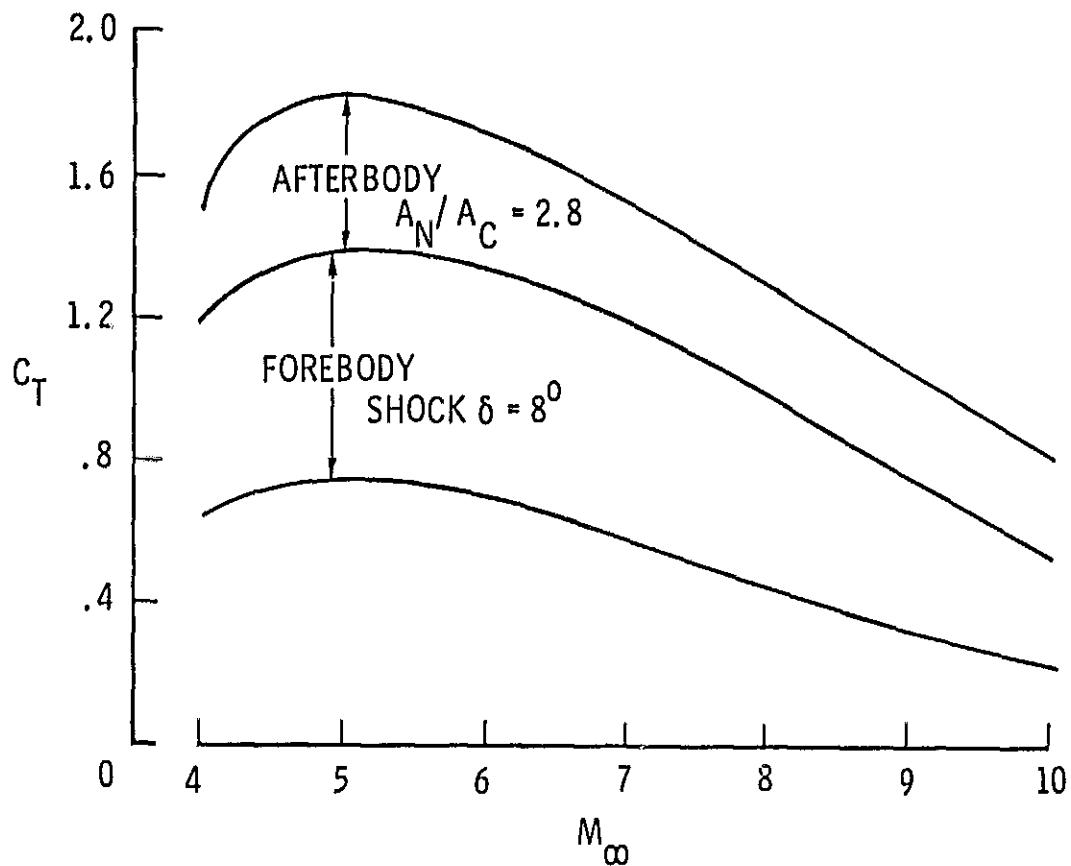
Figure 3.- Contributions of engine-airframe integration to thrust.
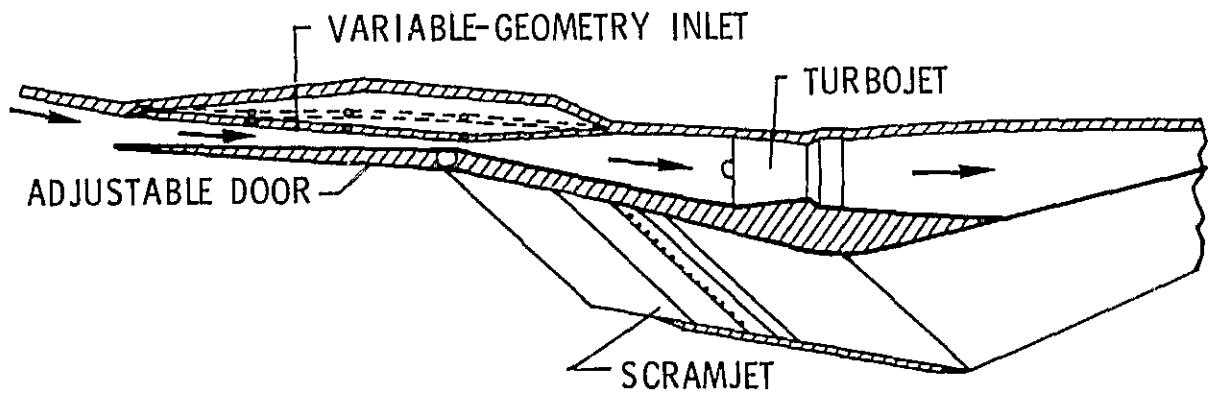
Figure 4.- Hypersonic propulsion system schematic.
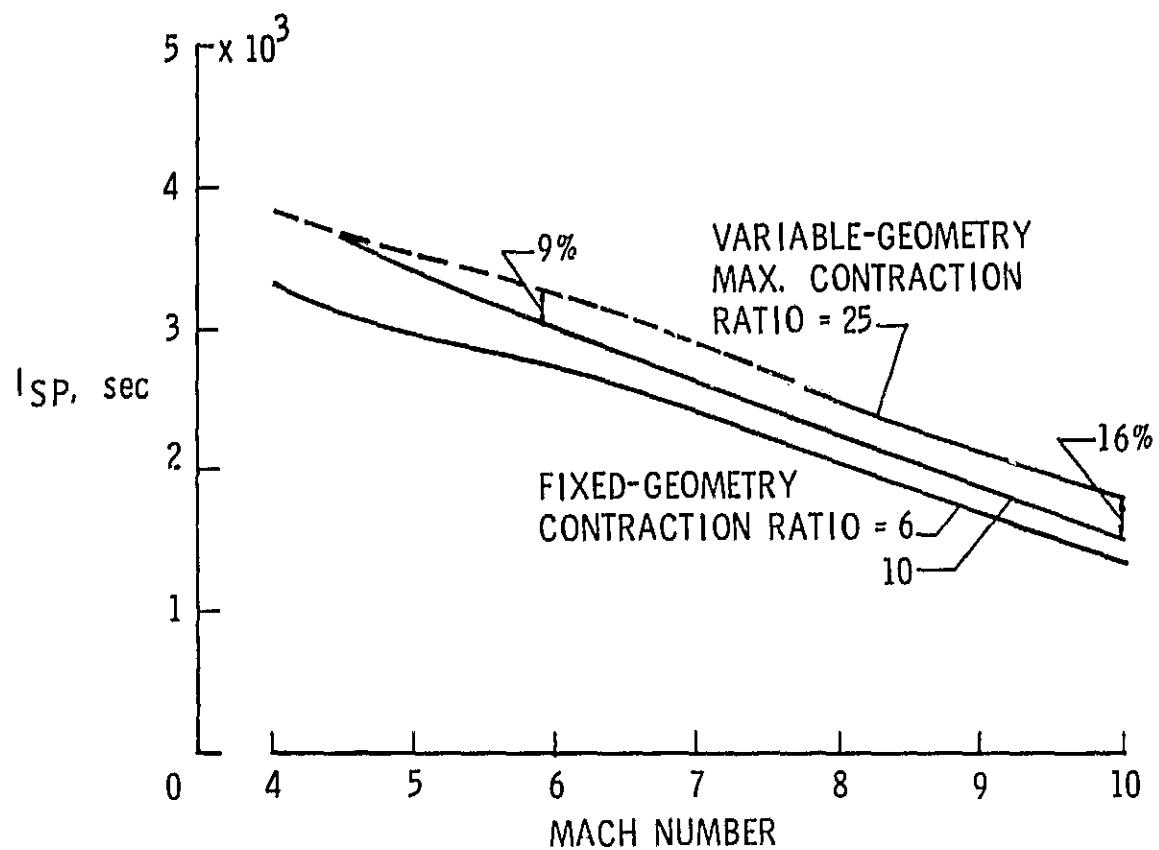
Figure 5.- Effect of inlet variable geometry.
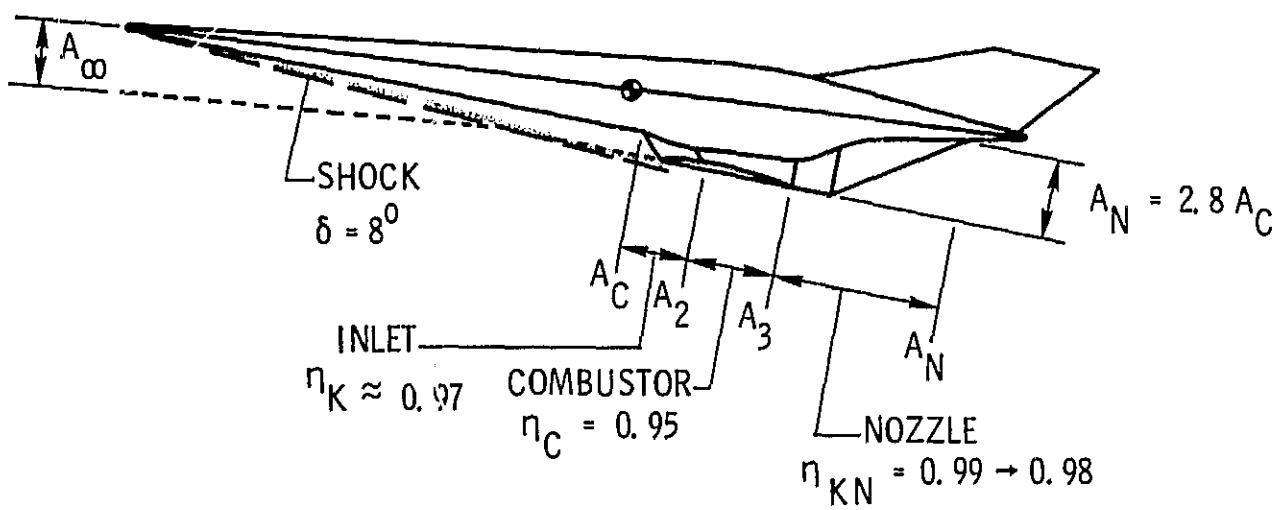
Figure 6.- Baseline assumptions. q_∞ = 47.9 kN/m^2 (1000 psf); ϕ = 1.0; A_C/A_2 = 10.
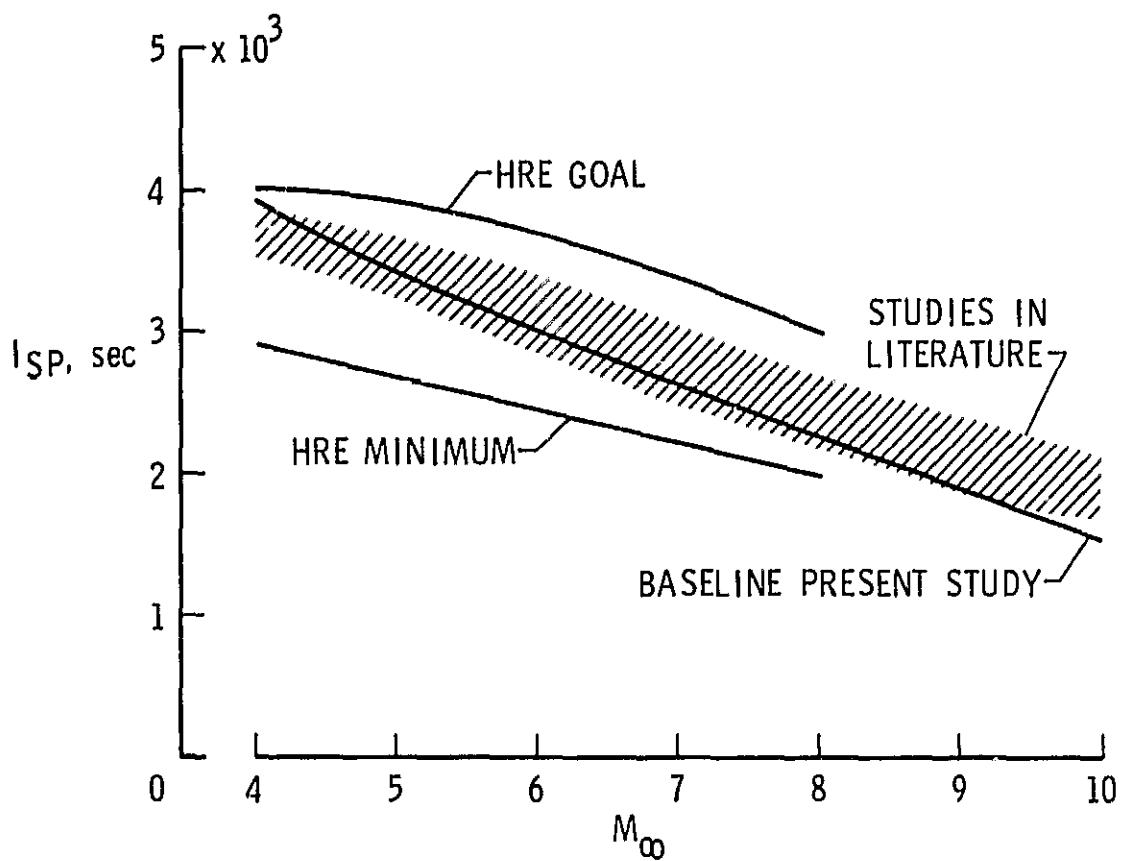
Figure 7.- Specific impulse comparisons.
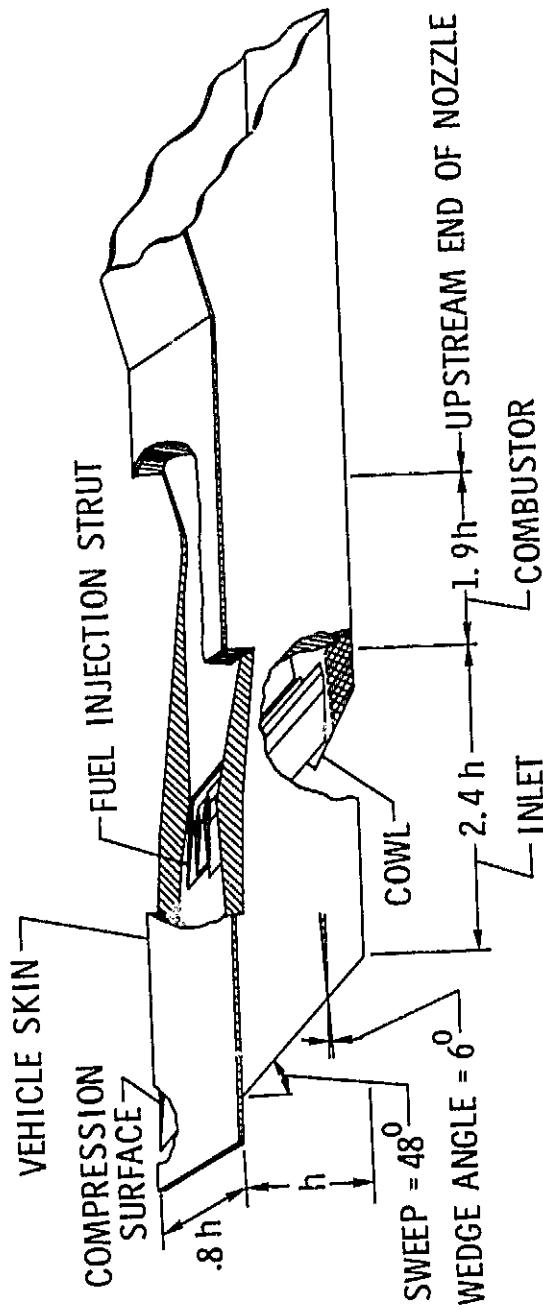
Figure 8.- Langley scramjet concept. Oblique view of inner module.
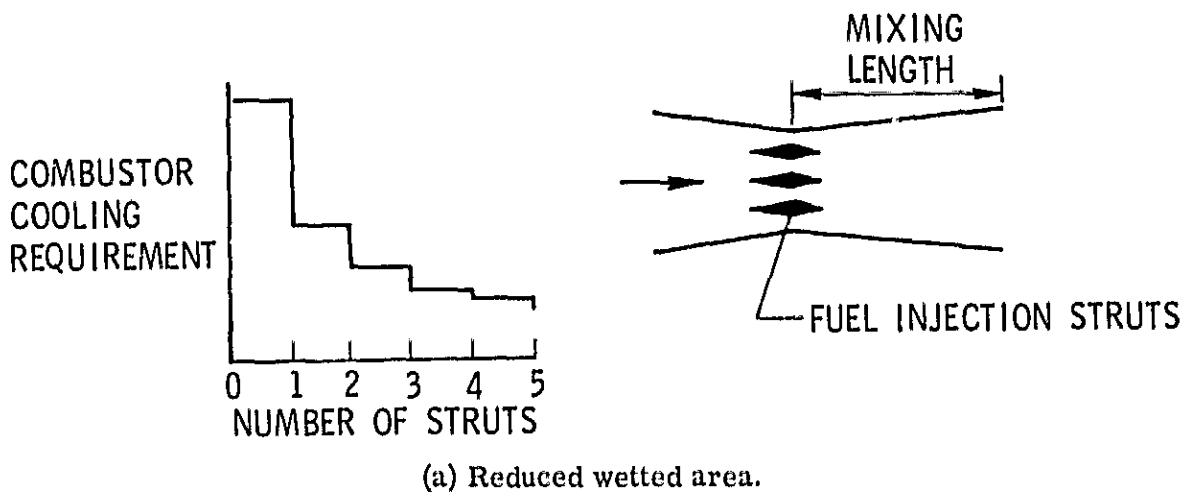
(a) Reduced wetted area.
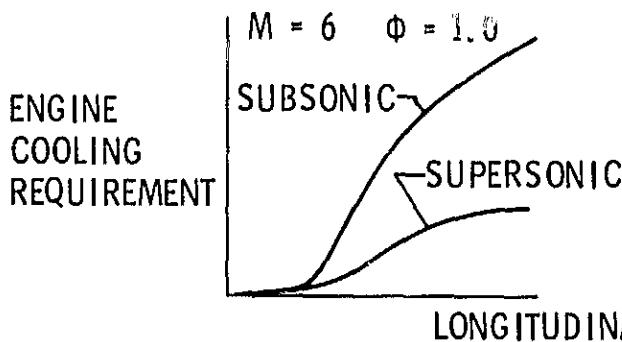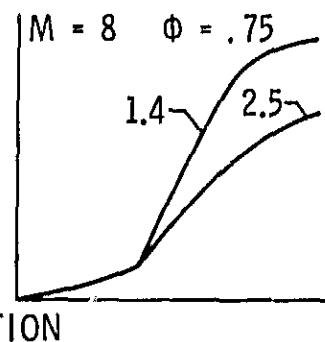
(b) Combustion mode.   (c) Combustor area ratio.

Figure 9.- Engine design features for reduced cooling requirements.
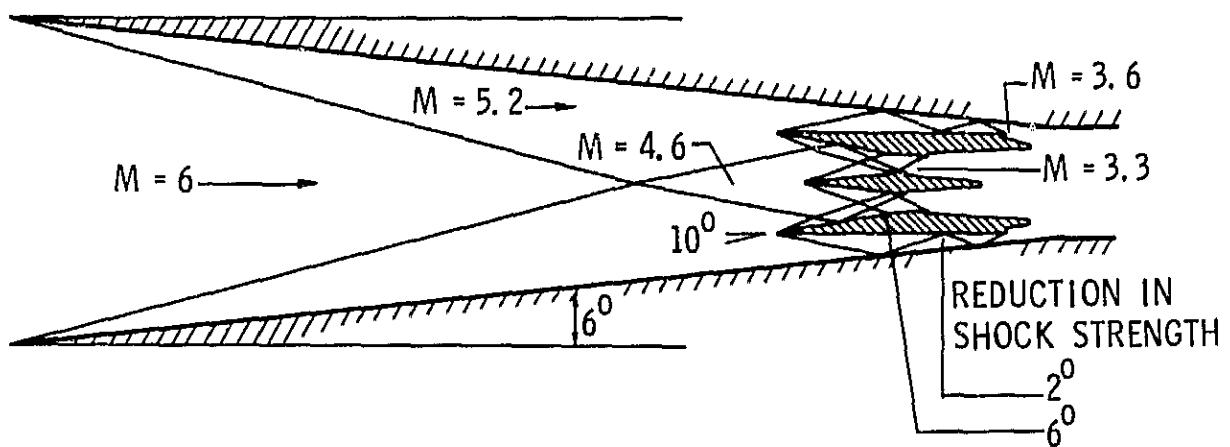
Figure 10.- Shock diagram. Langley scramjet concept. $M_{\infty} = 7.6$.
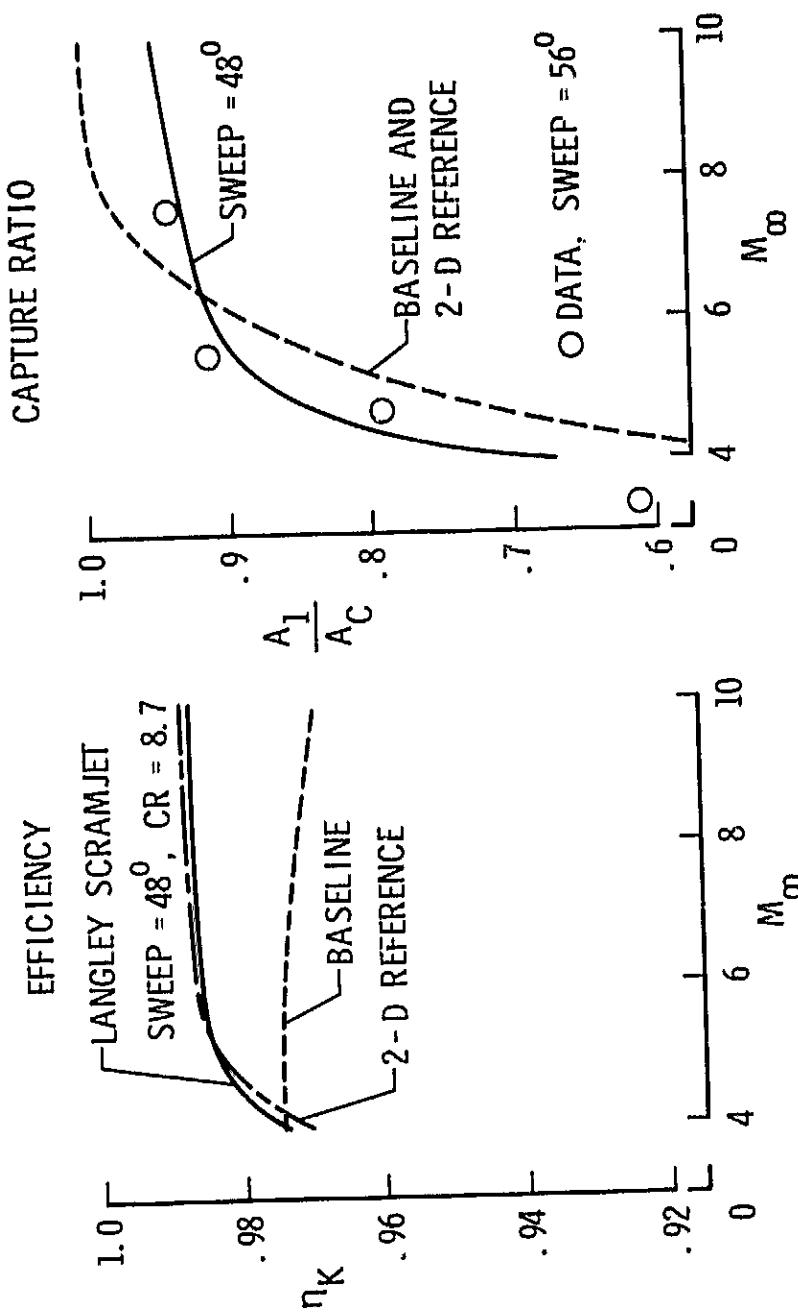
Figure 11.- Inlet performance analyses.
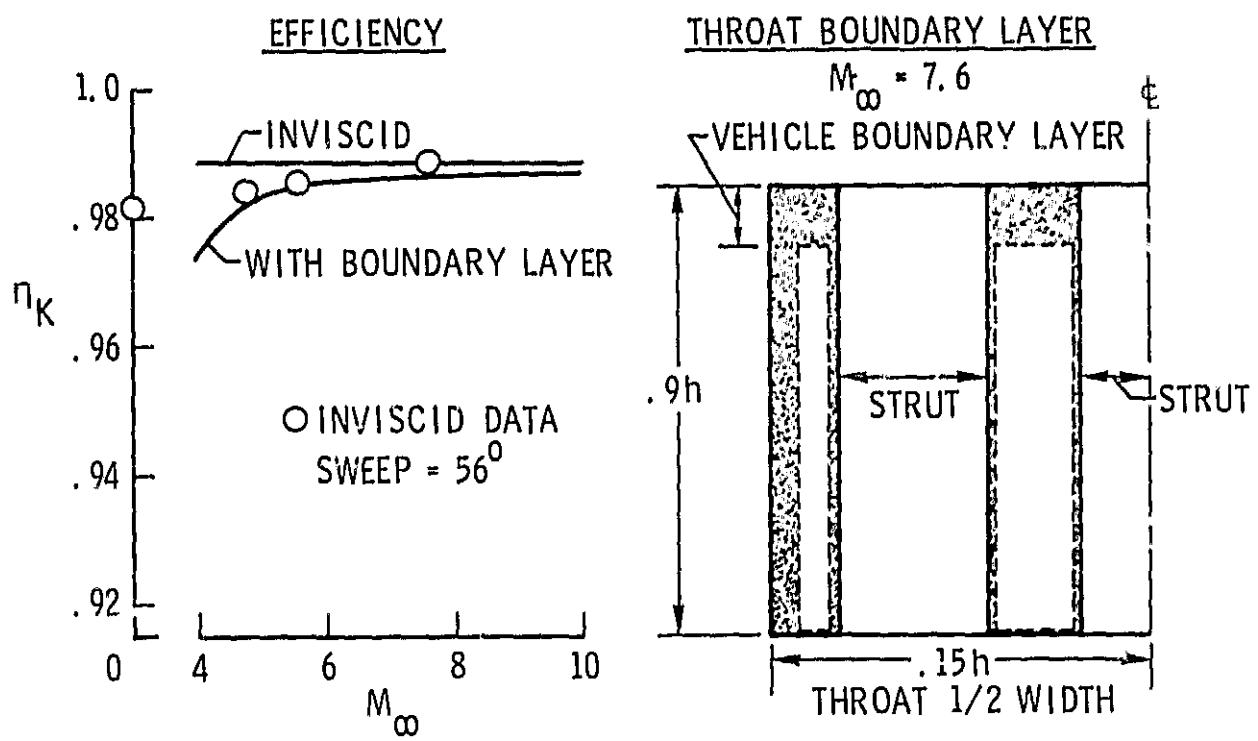
Figure 12.- Inlet performance analyses.   Langley scramjet.
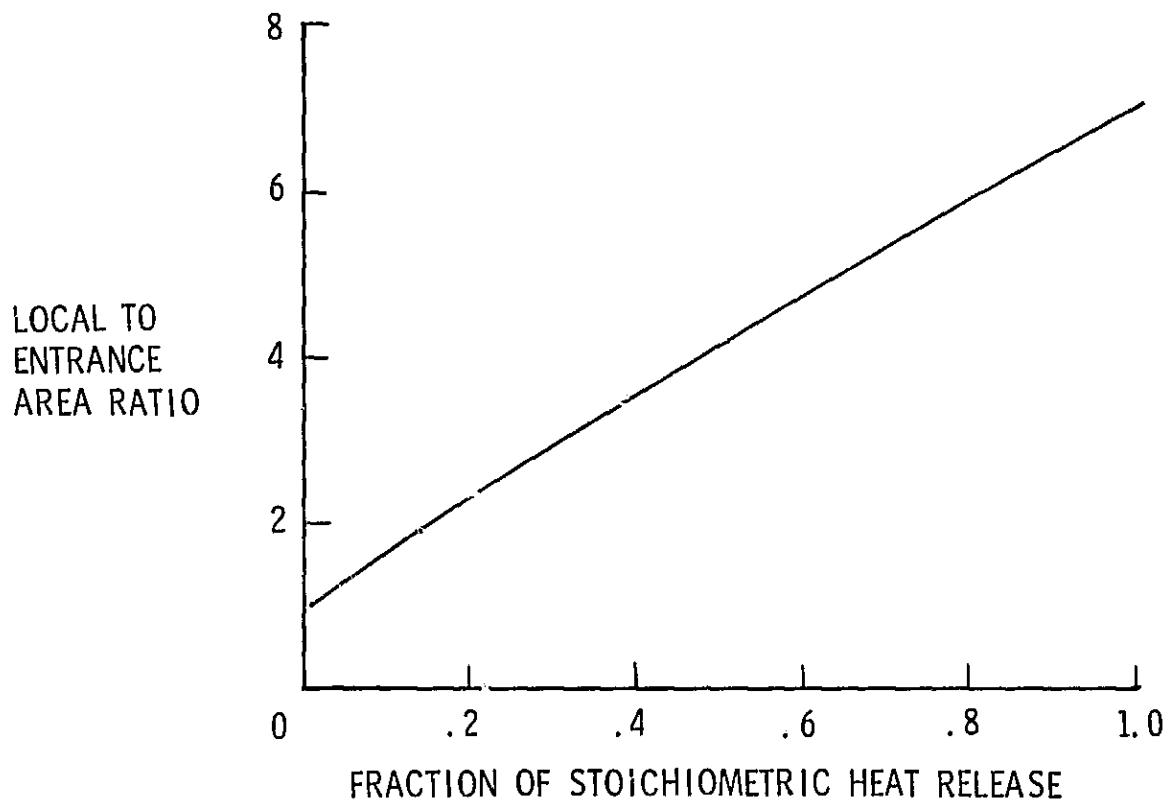
Figure 13.- Combuster area ratio, Mach 4 flight. Constant Mach number heat release.
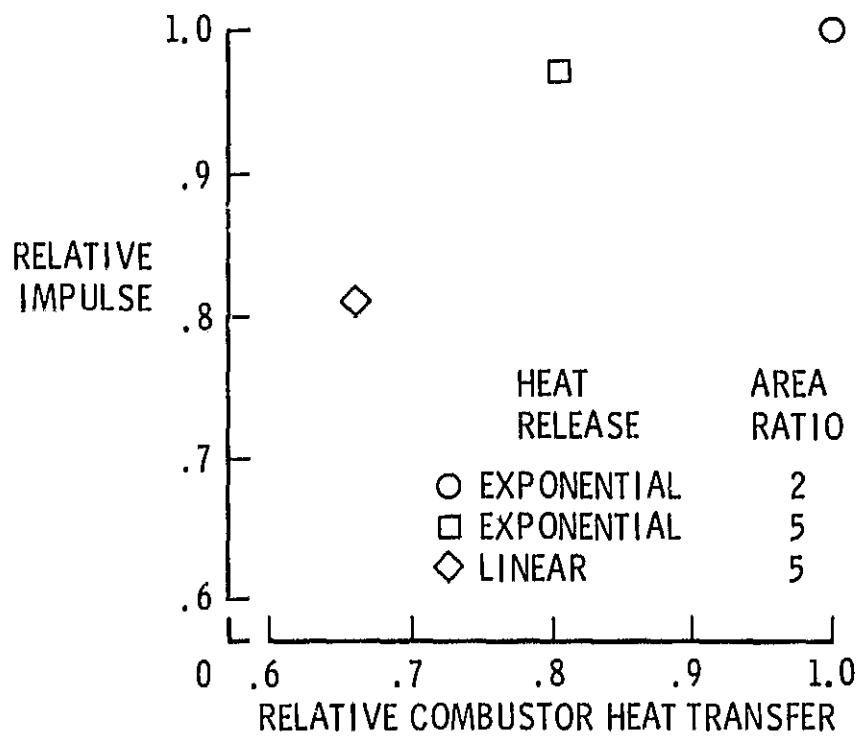
Figure 14.- Trade-off between impulse and cooling requirements.
Mach 10 flight; $\phi = 1.0$.
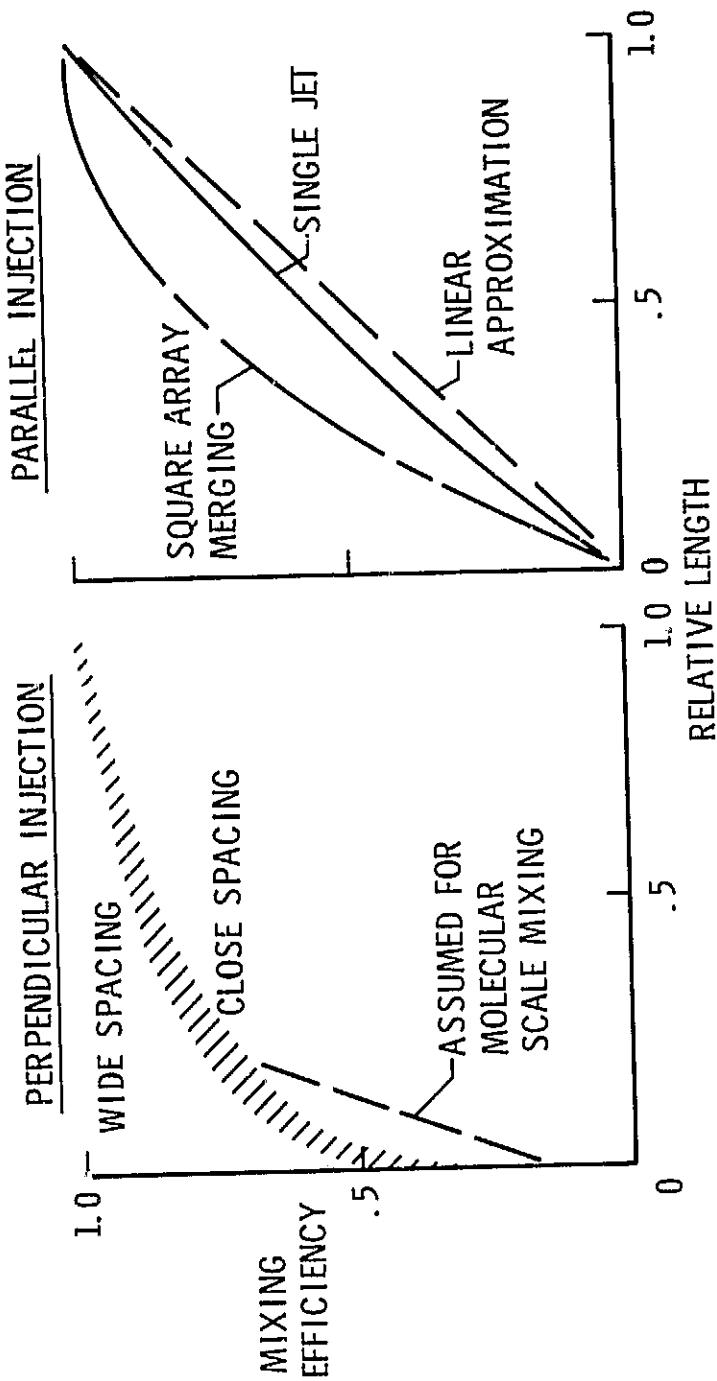
Figure 15.- Mixing efficiency distributions.
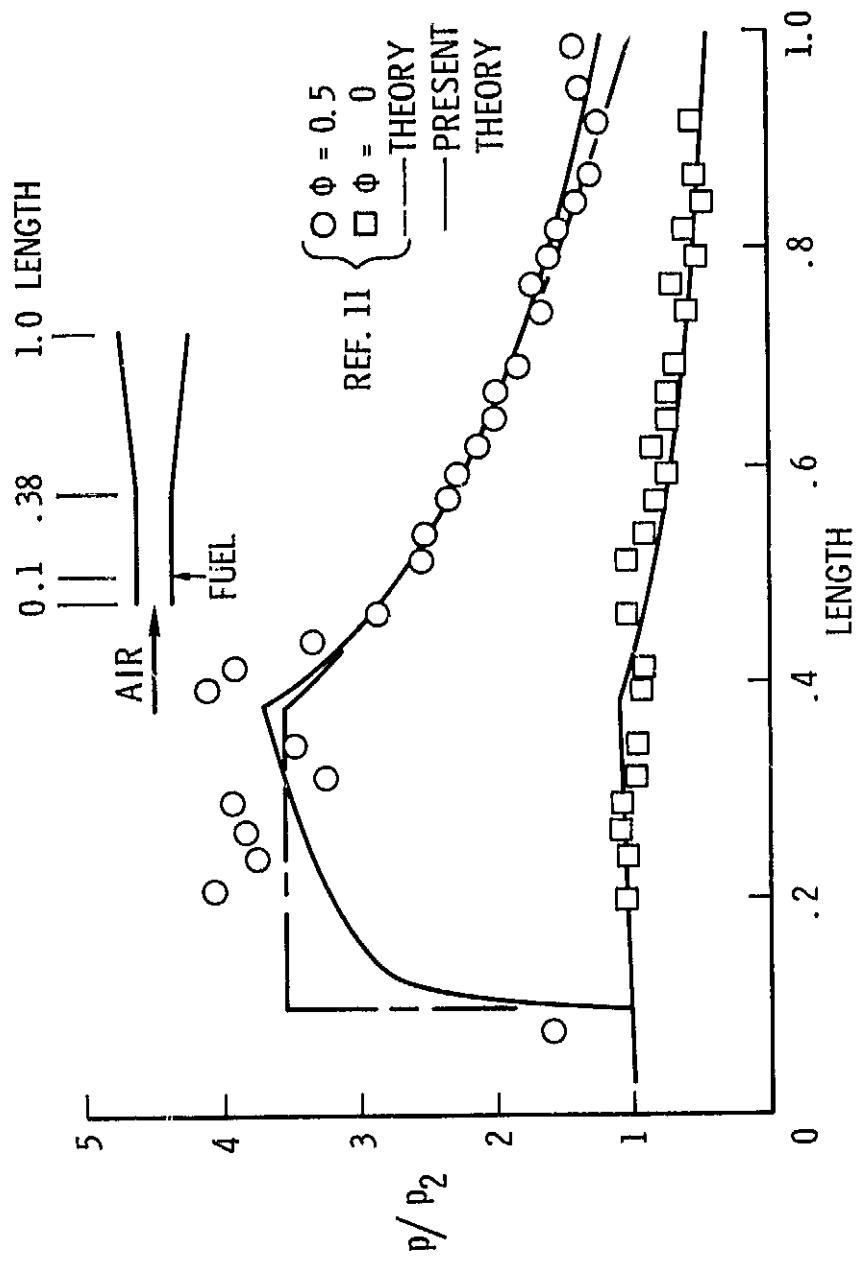
Figure 16.- Combustor static pressure distributions.
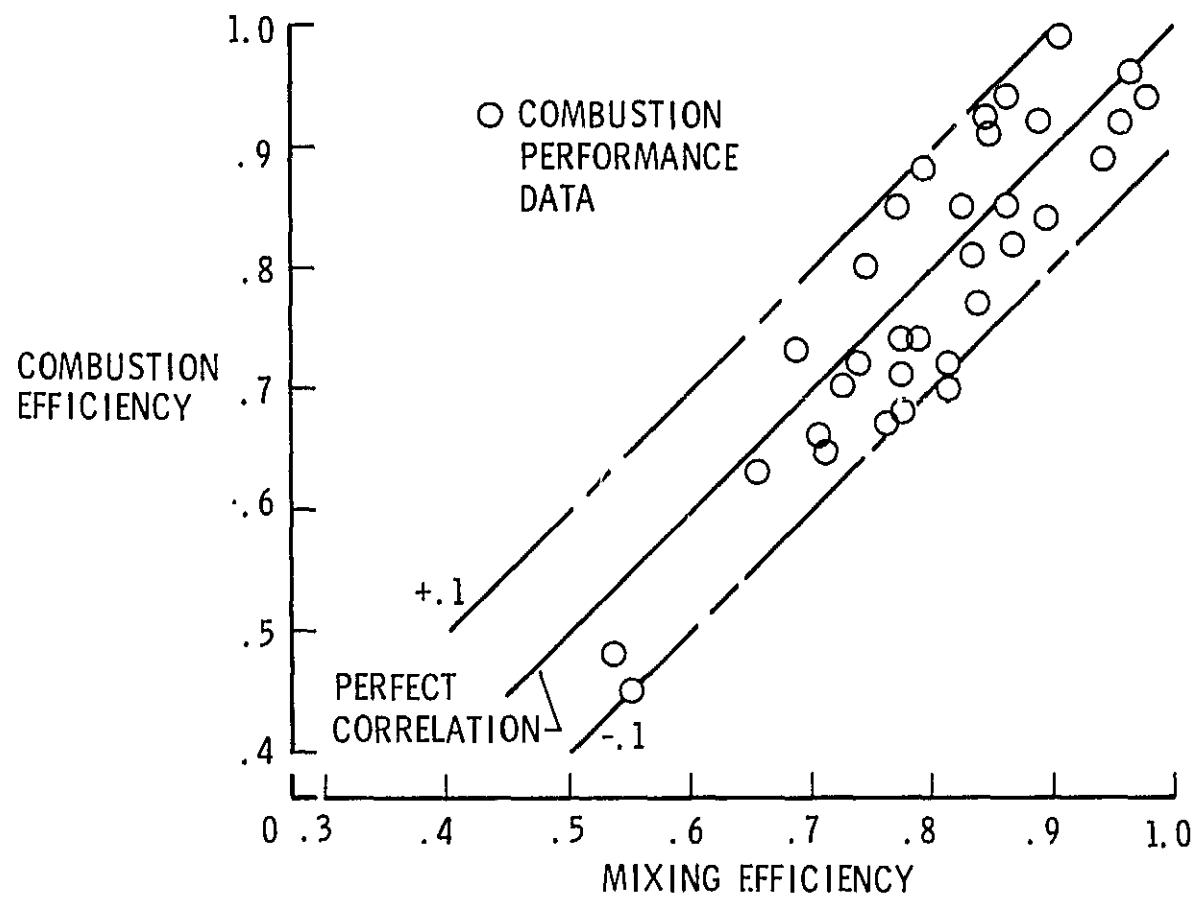
Figure 17.- Comparison of combustion and mixing efficiencies.
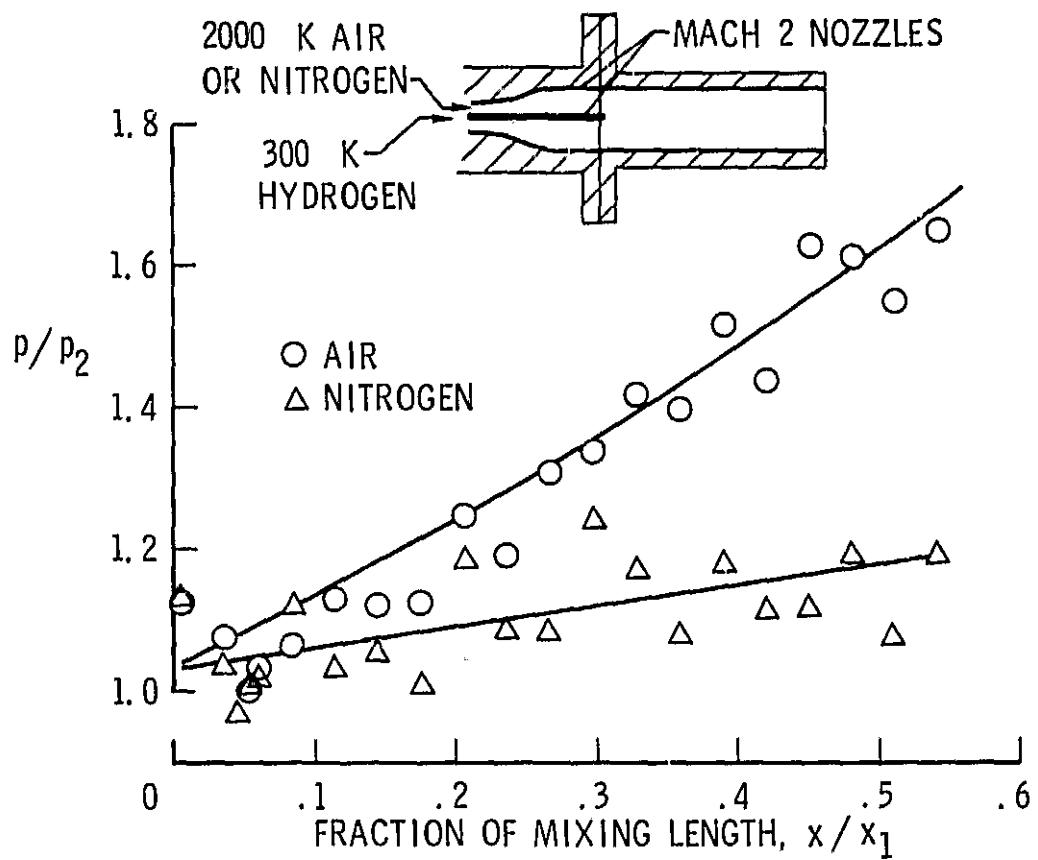
Figure 18.- Combustor static-pressure distributions.

FRONT VIEW   VIEW IN PLANE OF COWL
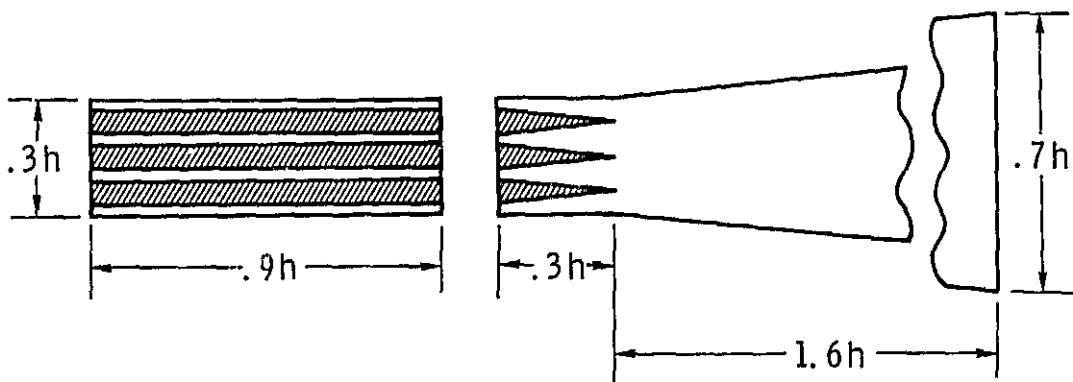
Figure 19.- Langley scramjet combustor design.
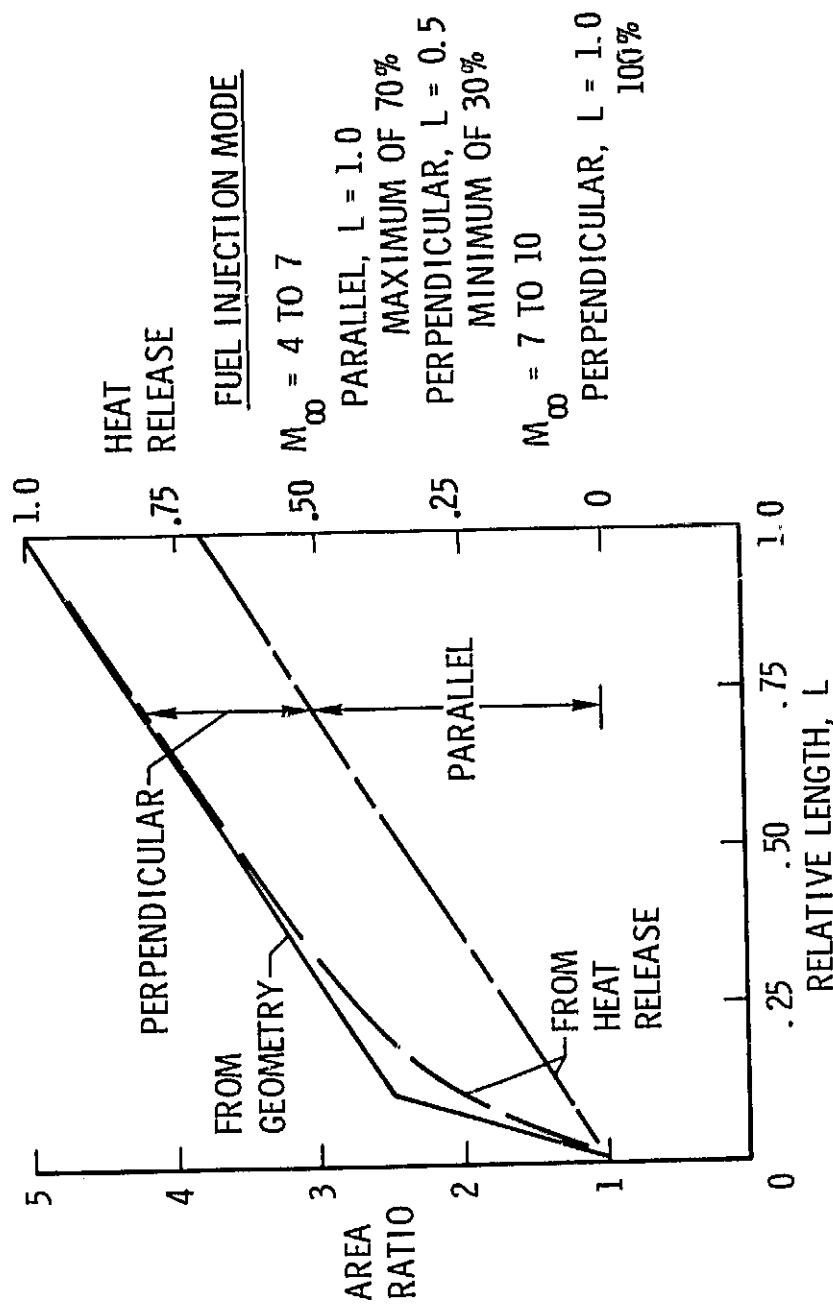
Figure 20.– Combustor heat release distribution.
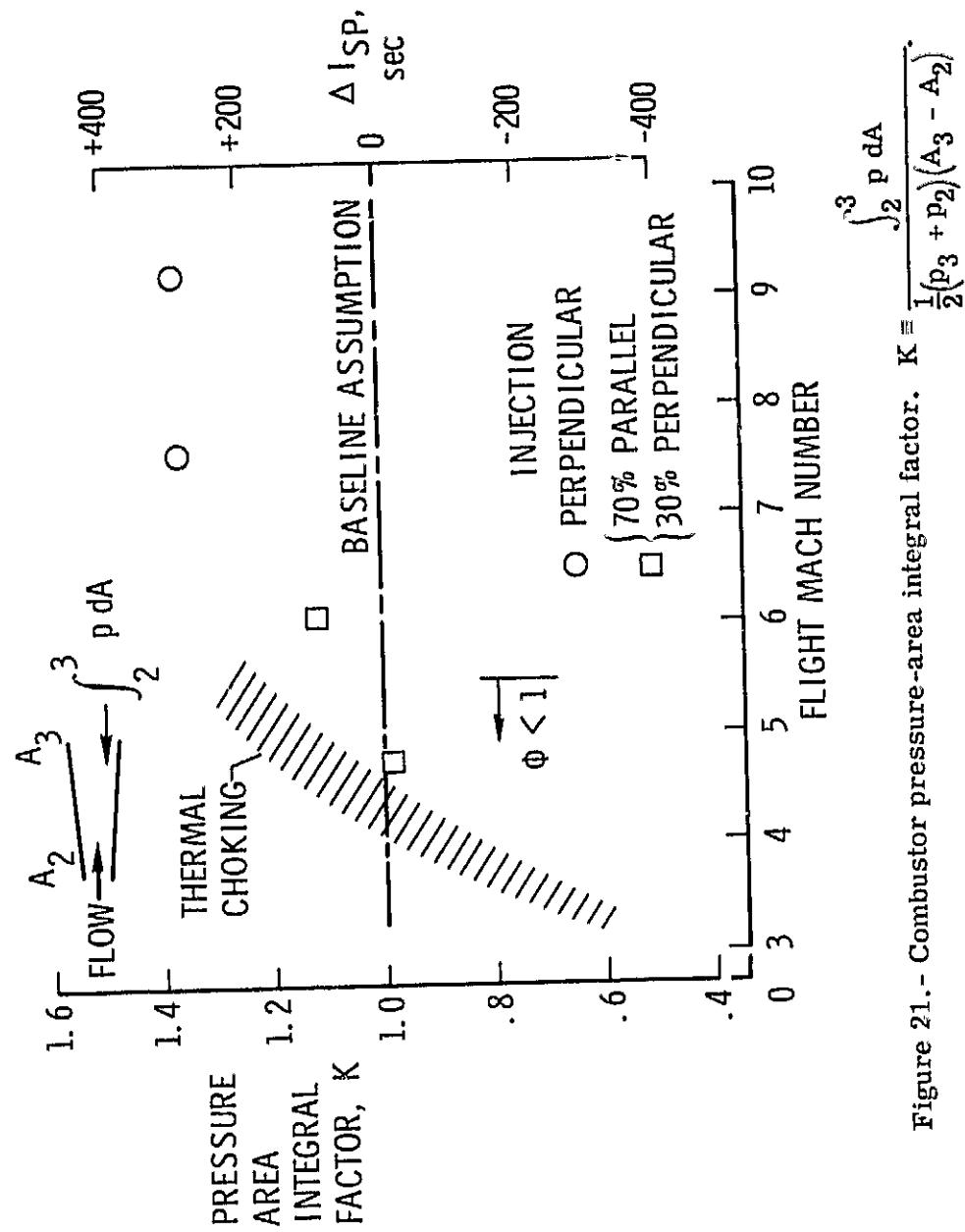
Figure 21.- Combustor pressure-area integral factor. $K \equiv \dfrac{\int_2^3 p\, dA}{\frac{1}{2}(p_3 + p_2)(A_3 - A_2)}$
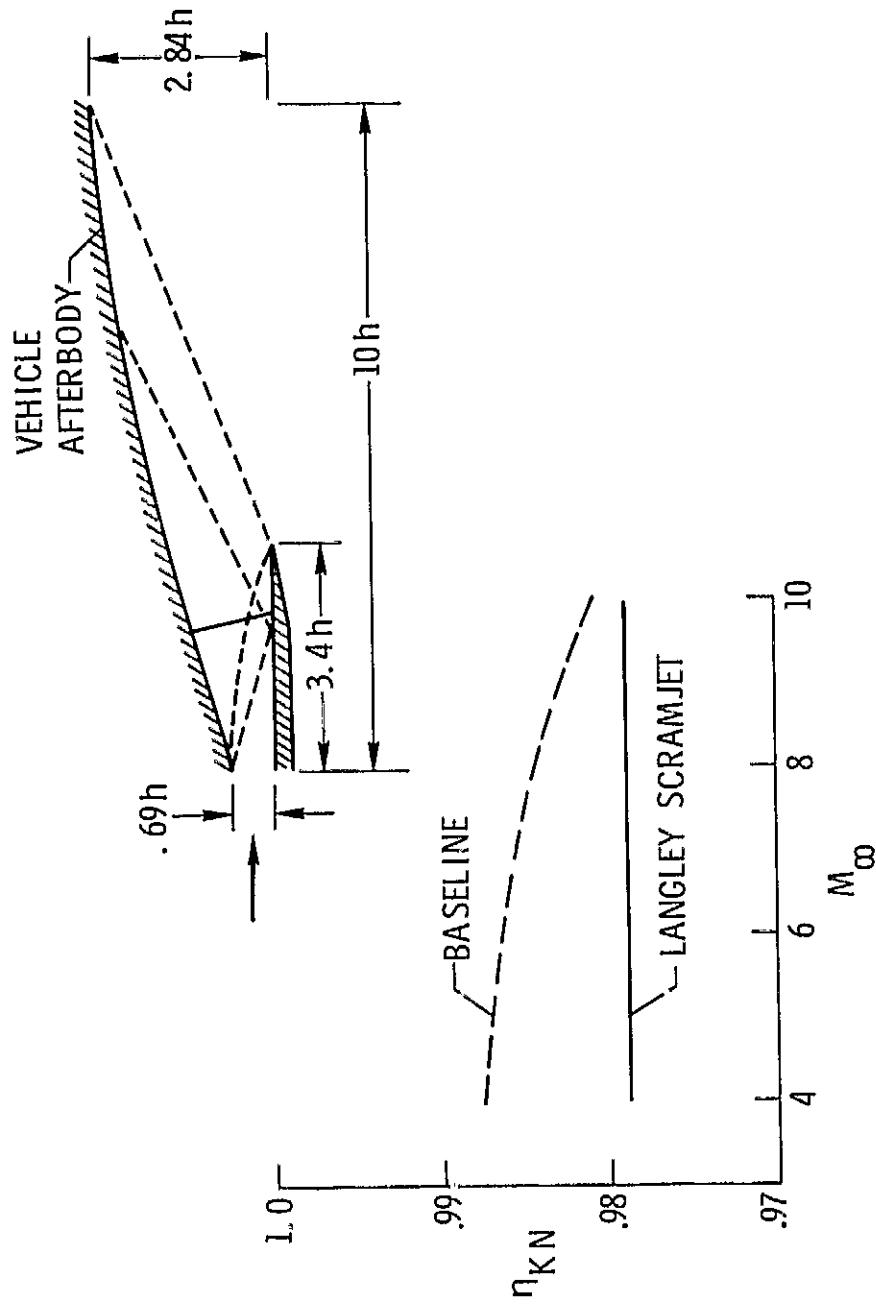
Figure 22.- Nozzle performance.
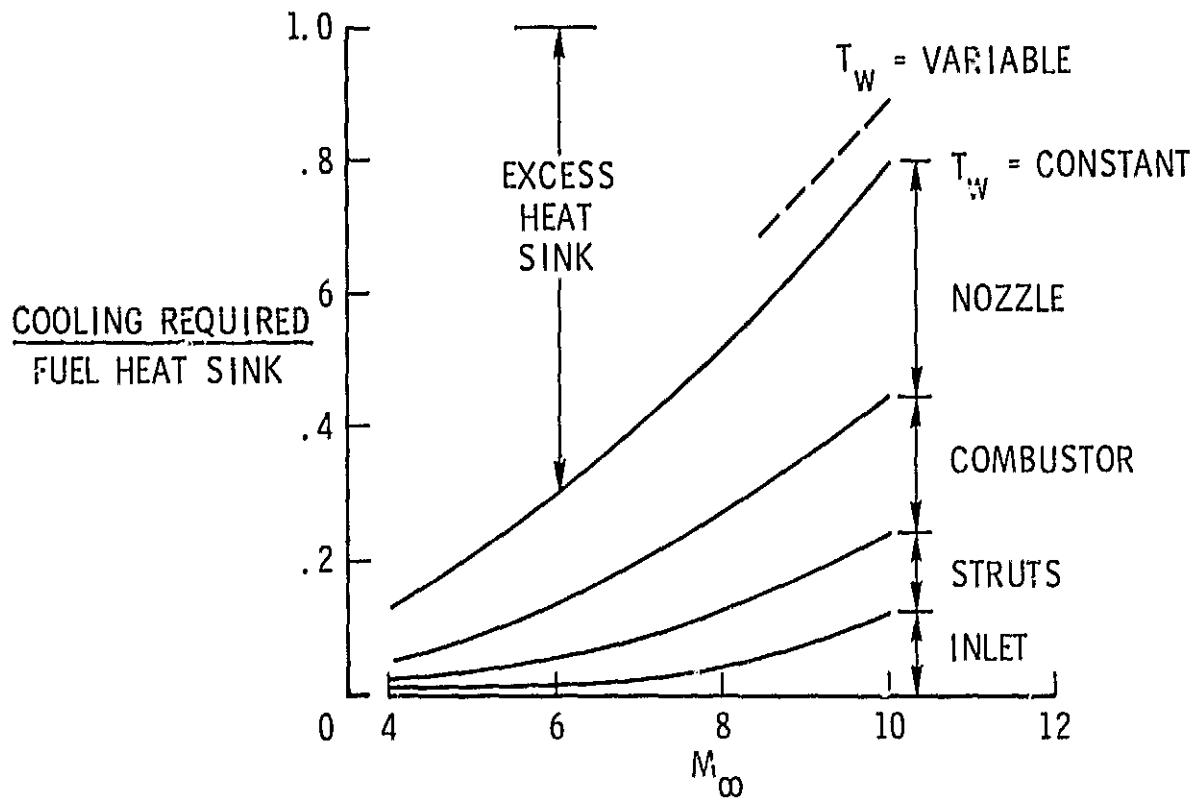
Figure 23.- Langley scramjet cooling required. $q_{\infty} = 47.9$ kN/m^2 (1000 psf); $\phi = 1.0$.
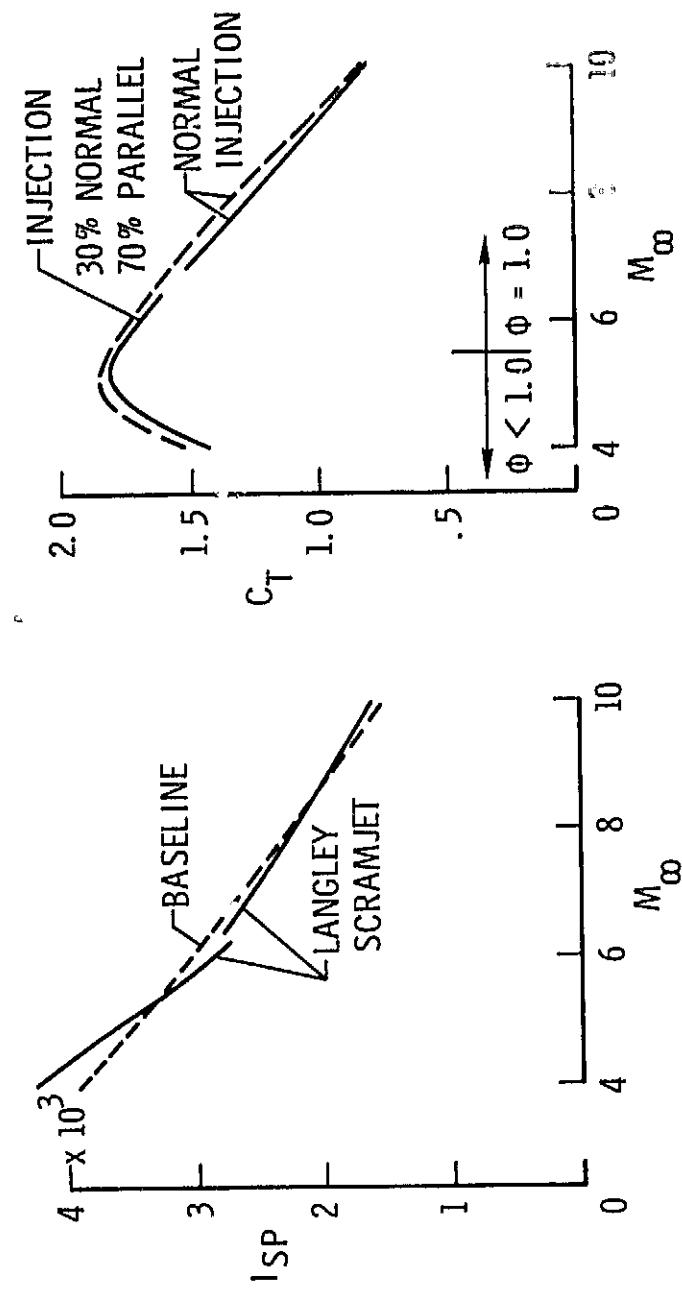
Figure 24.- Performance prediction.